

Manuscript submitted to EMMCVPR 2005

COVER PAGE

TITLE : Constrained Total Variation Minimization and Application
in Computerized Tomography

AUTHOR'S NAME : Xiao-Qun Zhang, Jacques Froment

CORRESPONDING AUTHOR : Jacques Froment

AFFILIATION : Université de Bretagne Sud

ADDRESS : LMAM, Université de Bretagne Sud, Campus de To-
hannic - Y. Coppens, BP573, 56017 Vannes, France

EMAIL ADDRESS : xiaoqun.zhang@univ-ubs.fr, Jacques.Froment@univ-
ubs.fr

FAX : +33 297017175

TELEPHONE NUMBER : +33 297017138

ABSTRACT : We present a simple framework for solving different ill-posed inverse problems in computer vision by means of constrained total variation minimizations. We argue that drawbacks commonly attributed to total variation algorithms (slowness and incomplete fit to the image model) can be easily bypassed by performing only a few number of iterations in our optimization process. We illustrate this approach in the context of computerized tomography, that comes down to inverse a Radon transform obtained by illuminating an object by straight and parallel beams of x-rays. This problem is ill-posed because only a finite number of line integrals can be measured, resulting in an incomplete coverage of the frequency plane and requiring, for a direct Fourier reconstruction, frequencies interpolation from a polar to a Cartesian grid. We introduce a new method of interpolation based on a total variation minimization constrained by the knowledge of frequency coefficients in the polar grid, subject to a Lipschitz regularity assumption. The experiments show that our algorithm is able to avoid Gibbs and noise oscillations associated to the direct Fourier method, and that it outperforms classical reconstruction methods such as filtered backprojection and Rudin-Osher-Fatemi TV restoration, in terms of both PSNR and visual quality.

Constrained Total Variation Minimization and Application in Computerized Tomography

Xiao-Qun Zhang** and Jacques Froment

LMAM, Université de Bretagne Sud, Campus de Tohannic - Y. Coppens, BP573,
56017 Vannes, France

Abstract. We present a simple framework for solving different ill-posed inverse problems in computer vision by means of constrained total variation minimizations. We argue that drawbacks commonly attributed to total variation algorithms (slowness and incomplete fit to the image model) can be easily bypassed by performing only a few number of iterations in our optimization process. We illustrate this approach in the context of computerized tomography, that comes down to inverse a Radon transform obtained by illuminating an object by straight and parallel beams of x-rays. This problem is ill-posed because only a finite number of line integrals can be measured, resulting in an incomplete coverage of the frequency plane and requiring, for a direct Fourier reconstruction, frequencies interpolation from a polar to a Cartesian grid. We introduce a new method of interpolation based on a total variation minimization constrained by the knowledge of frequency coefficients in the polar grid, subject to a Lipschitz regularity assumption. The experiments show that our algorithm is able to avoid Gibbs and noise oscillations associated to the direct Fourier method, and that it outperforms classical reconstruction methods such as filtered backprojection and Rudin-Osher-Fatemi TV restoration, in terms of both PSNR and visual quality.

1 Introduction

Many ill-posed problems in computer vision may be solved by minimizing the total variation (TV) of an image, subject to a constraint : the TV functional provides an appropriate solution to the visual perception, while the constraint ensures that the solution satisfies all the conditions stated in the problem.

1.1 The total variation and the Rudin-Osher-Fatemi approach

If the image f is defined on the bounded, open and convex region Ω of \mathbb{R}^2 such that $f \in L^1(\Omega)$, one sets

$$\text{TV}(f) := \int_{\Omega} |\nabla f| dx \quad (1)$$

** X. Zhang is partially supported by *La Région Bretagne* under grant B/1042/2003/300/MIRIM.

where ∇f is the weak gradient of f that is, the vector of the partial derivatives of f taken in the distributional sense. The set of functions of Bounded Variation (BV) is defined as the Banach space of L^1 functions with finite TV, using the TV-seminorm.

The TV functional has been first introduced by Rudin, Osher and Fatemi (ROF) in [1] in the context of image denoising. It has proved to be particularly relevant in recovering piecewise smooth functions without smoothing sharp discontinuities (edges). The ROF problem is formulated in the constraint minimization form by

$$\inf_f \text{TV}(f) \quad (2i) \quad \text{subject to} \quad \int_{\Omega} (o - f)^2 = \sigma^2 \quad (2ii), \quad (2)$$

where o is the observed image, which is assumed to be corrupted by a Gaussian noise of variance σ^2 . Introducing a Lagrange multiplier λ , (2) is equivalent to the following unconstrained minimization problem [2], that can be viewed as a particular Tikhonov regularization :

$$\inf_f \text{TV}(f) + \lambda \int_{\Omega} (o - f)^2. \quad (3)$$

The ROF algorithm consists in solving (3) by using a time marching scheme to reach the steady state of a nonlinear diffusion process. The parameter $\lambda \geq 0$ in the data-fidelity term is chosen so that the constraint (2ii) is satisfied. Unfortunately such choice is not always possible, leading to a solution not consistent with the problem. Notice that to avoid non-differentiability of the TV-functional in constant areas, a small perturbation is added. This may significantly alter the original energy functional.

1.2 Following developments

The introduction of the ROF algorithm has been of great interest in image denoising and deblurring, and recent years have seen number of developments of TV-minimization methods. Lot of work has been done to obtain more efficient minimization algorithms or better mathematical properties, most often by slightly modifying the TV functional to ensure differentiability [3][4][5][6][7][8], by using level sets thanks to the Coarea formula [9][10], or more recently by using subgradients methods [11][12][13]. The ROF approach has also been enlarged to various restoration problems, sometimes in combination with cosine or wavelets bases [14][15][16][17][18]. A few authors have proposed to enhance the TV model by using a more appropriate norm in the fidelity constraint. The l_1 norm can be found in [19] in relation with recursive median filters. In [20][21], M. Nikolova uses a l_1 data-fidelity term that involves an implicit detection of outliers. An exact optimization scheme in the case of L^1 or L^2 norms is given in [10].

A major deception in the mathematical image processing community was to discover that the BV space is still not the appropriate space to model physical images : natural images are not, in general, of finite TV because of microtextures

generating oscillations at every scales [22]. In order to measure textural parts removed by the TV functional, Y. Meyer has introduced in [23] a dual norm called the G-norm and he has proposed to use it for the data-fidelity term. This was the beginning of promising researches for new dual norms [24][25] and new functionals allowing the decomposition of the image f into $f = u + v + w$ where u is the cartoon-part (detected by minimizing the TV), v the textural part, and where the residue w contains the undesirable noise [26][27].

1.3 Our contribution

In this article, we present a constrained TV-minimization framework that we believe to be mathematically and numerically simple, flexible enough to be used to solve various ill-posed inverse problems in computer vision, and that avoids the main drawbacks commonly attributed to TV-minimization : slowness of basic gradient algorithms and incomplete fit to the image model. Such a framework has already been applied by one of us, together with S. Durand and F. Alter, to denoise signal using wavelet shrinkage [12] and to restore JPEG-compressed images [28]. One of the main goal of this present article is to emphasize that a complete mathematical model of images may not always be necessary, nor even suitable, to obtain efficient image reconstruction or restoration algorithms. Indeed, a solution of a formal optimization problem is numerically found as the result of an iterative procedure when the number of iterations tends to infinity. Therefore, the practitioner is facing the following choice : should I try to obtain a good approximation, and then to keep the algorithm running a long time, or should I perform only a small number of iterations, to preserve a low computational complexity ? We claim that the BV space, as an incomplete image model unable to contain the thinnest details, should sometimes be seen as a chance to build algorithms with best results after a small number of iterations only (typically less than 10, see Fig.3).

After these remarks, we introduce our main original contribution : an application of our constrained TV-minimization framework to Computerized Tomography (CT). CT is the typical ill-posed inverse problem in image reconstruction. Besides, obtaining noiseless high quality tomographic images in limited time (low hardware cost) is of great importance for improving public health. A CT scanner contains a rotating x-ray device to create cross-sectional images of the body. The input is the set of x-ray projections called sinogram and which corresponds to the Radon transform of the image f that has to be reconstructed. If the Radon transform can be theoretically inverted using Fourier transforms, it requires however a complete set of projections. In practice only a finite number of projections can be measured, resulting in an incomplete coverage of the frequency plane. Solving the CT problem involves therefore to perform (implicitly or explicitly) a frequency interpolation, from a polar to a Cartesian grid. This is the critical point of CT. As far as we know, it does not exist any CT interpolation method based on a mathematical model that tell us what should be the reconstructed image in accordance with the visual perception. As a result of, the two main families of reconstruction methods, direct Fourier methods

(DFM) and filtered backprojection (FBP), generate visual artefacts : DFM are by far those suffering worse artefacts, with unpleasant oscillations due to noisy data in high frequencies. In presence of noise, the performance of FBP is fair since it consists of averaging backprojections for all sinogram lines. Moreover, a Hamming window is often applied to deemphasize high frequencies. This explains why windowed FBP is currently considered as the best reconstruction method. However, windowed FBP is unable to remove the noise while keeping edges sharp. We claim that the BV model is particularly adapted to model CT images. No doubt, as for other images, the TV is not able to model the finest details. However, CT scanners cannot deliver very thin details as they are mixed with the noise. The technology seems not ready to offer textured CT images, and the common test image is still the famous Shepp-Logan phantom [29], an image made by piecewise-constant functions (for which level lines are ellipses).

In the constrained TV-minimization framework applied to CT, the key point is to define the constraint space. The solution we are currently proposing is based on a local Lipschitz regularity assumption of the Fourier spectrum. From the input data in the polar grid, we compute the local Lipschitz constants and we assume that, locally, those constants are the same in the Cartesian grid. This allows to set intervals of frequency values in the Cartesian grid, resulting in defining the constraint as a frequency hypercube. Following our constrained TV-framework, the numerical scheme performs a subgradient “descent” combining a projection on this hypercube. The method does converge, but the practitioner is warned not to try to reach the convergence zone. Indeed, and this seems to be a characteristic shared by all instantiations of our constrained TV-framework, the first iterations of the subgradient algorithm make edges sharper while removing the noise but not meaningful structures. If too many iterations would be performed, the constraint space may be too large to avoid loss of thin details, and the visual quality of the solution would decrease. As a result of, the numerical scheme is pretty fast and remain of the same order than the classical methods DFM and FBP. However, the reconstructed image is of better quality both visually and in term of PSNR.

2 A simple constrained-TV framework

2.1 The subgradient projection method

As noted before, the ROF method is implemented using the unconstrained minimization (3), and it does not guarantee the condition (2ii) to be satisfied. In addition, the practitioner has to deal with the parameter λ . By explicitly defining a set $U \subset \text{BV}$ of admissible solutions, we avoid such drawbacks and the formulation is more flexible than the one based on a data-fidelity term. The set U models the knowledge on the image, computed from the input data. In the following, we will assume U to be a convex set. The constrained optimization problem can be simply written as

$$\text{find } f^* \in U \quad \text{such that } \text{TV}(f^*) = \min_{f \in U} \text{TV}(f). \quad (4)$$

In the numerical analysis of the TV minimization, the difficulty comes from the non-differentiable argument $|\nabla|$. Most authors introduce a form of relaxation as

$$\text{TV}(f) = \int_{\Omega} \sqrt{|\nabla f|^2 + \beta} \, dx \quad (5)$$

where β is a small positive parameter [5][6][7][8]. However, by smoothing the TV functional one loses more or less the main advantage of the BV model: allowing restoration of sharp discontinuities. This smooth approximation approach has other serious shortcomings, see [11] for details. Therefore, as some other authors [4][11][13][30], we propose to compute the TV without any regularization and to overcome the singularity, we adjust the standard gradient descent algorithm to subgradients.

Since TV is a convex function and U a convex set, any solution f^* of (4) is given by

$$t > 0, \quad f^* = P(f^* - t \cdot g(f^*)), \quad (6)$$

where P is the projector onto U that minimizes the distance and $g(f)$ a subgradient of $\text{TV}(f)$ at f . This equation leads to the following iterative process, known as Polyak's subgradient projection method [31] [11] :

$$f^{k+1} = P(f^k - t_k g(f^k)), \quad t_k > 0, \quad f^0 \in U. \quad (7)$$

A classical condition to ensure the convergence of this algorithm is for step-sizes $(t_k)_k$ to converge to zero not too rapidly [31][28] :

$$\text{If } \sum_{k=0}^{+\infty} t_k = +\infty \text{ and } \sum_{k=0}^{+\infty} t_k^2 < +\infty, \text{ then } \exists f^* \in U / \lim_{k \rightarrow +\infty} f^k = f^*. \quad (8)$$

As a result of, the subgradient projection method is considered as a slow algorithm and several strategies may be developed to speed it [11]. However our opinion is that, in the context of constrained TV-minimization, this point is not crucial since the practitioner would have advantage to stop the algorithm after a few number of iterations.

2.2 A simple algorithmic framework

A more annoying point is the computation of the projection $P(f)$. When it cannot be implemented in a straightforward fashion, it requires sophisticated algorithms that can be time-consuming (see works of P. Combettes [32][11]). Our simple constrained-TV framework is obtained by noticing that various ill-posed inverse problems in computer vision involve an orthogonal linear transform T applied on pixel's values. If f is a discrete image of size $N \times N$, one introduces

$$T : \mathbb{R}^{N^2} \rightarrow \mathbb{R}^{N^2}, \quad T \in \text{Orthogonal group of } \mathbb{R}^{N^2}. \quad (9)$$

If the knowledge on the data is given in the domain $T(f)$, one may define the constraint set as

$$U = \left\{ f \in \mathbb{R}^{N^2} : (T(f))_n \in [T_n^-, T_n^+] \quad \forall n \in I \right\}, \quad (10)$$

where $I \subset \{1, \dots, N\}^2$ is a set of indices and where T_n^-, T_n^+ are fixed, depending of the input data only. With such a constraint the computation of the projection is straightforward, and the method leads the following simple, although general, algorithm:

1. Get $f^0 \in U$, usually by running a basic existing algorithm;
2. Choose a maximal (small) number of iterations K ;
3. Choose t_k , for example (but not necessarily) according to (8), e.g. $t_k = 1/(k+1)$;
4. Compute $v^k = f^k - t_k g(f^k)$;
5. Compute $w^k = T(v^k)$;
6. Set any $(w^k)_n < T_n^-$ to T_n^- , set any $(w^k)_n > T_n^+$ to T_n^+ ;
7. Set $f^{k+1} = T^{-1}(w^k)$;
8. Increment k ; loop to step 3 while $k < K$.
9. End. The result is the image f^K .

2.3 Examples

The specific form of the constraint U in (10) may be seen very restrictive. However in low-level computer vision, number of approaches involves the use of an orthogonal transform to process the image. Here are some examples we have successfully implemented, and which significantly improve existing algorithms.

Image denoising. This is the most basic example, in the spirit of the ROF algorithm. Assume that the observed image o is corrupted by a noise of variance σ^2 . Set $f^0 = o$, $T = \text{Identity}$, $I = \{1, \dots, N\}^2$, $T_n^- = o_n - 2\sigma$, $T_n^+ = o_n + 2\sigma$.

Signal denoising via wavelet shrinkage [33][12]. Signal (or image) denoising by means of a wavelet shrinkage consists of decomposing the noisy data o into a orthogonal wavelet basis, suppressing the wavelet coefficients smaller than a given amplitude, and transforming the data back into the original domain [34]. Let f^0 be the noiseless signal obtained in this way. To remove visual artefacts due to missing wavelet coefficients set $T = \text{orthogonal wavelet transform}$, $I = \text{map of the retained wavelet coefficients}$, $T_n^- = T_n^+ = (T(o))_n$.

JPEG restoration [14][28]. The observed image o has been compressed by the JPEG lossy coder [35]. To remove blocking artefacts and Gibbs oscillations due to a compression at low bit rates, set $f^0 = \text{decoded JPEG image}$, $T = \text{block cosine transform}$, and compute T_n^-, T_n^+ from the quantization table given in the bit-stream such that

$$(T(h))_n \in [T_n^-, T_n^+] \quad \forall n \in \{1, \dots, N\}^2, \quad (11)$$

for h the original (unknown) image.

3 Application in Computerized Tomography

Our main original contribution is in the following : we provide another example of our simple framework in the context of CT.

3.1 Computerized tomography issue

In CT the observed body slice is modeled as a two-dimensional distribution $(x, y) \mapsto f(x, y)$ of the x-ray attenuation constant, and a line integral called projection represents the total attenuation suffered by a beam of x-ray as it travels through the body. The line integrals are measured to approximate the distribution of the object. Let (r, θ) be such a line, r being the perpendicular distance from the line to the origin and θ the angle between the perpendicular vector and the x -axis. A projection obtained by illuminating the object along the line is given by

$$P_\theta(r) = \int_{(r,\theta)} f(x, y) dx dy = \int_{-\infty}^{\infty} \int_{-\infty}^{\infty} f(x, y) \delta(x \cos \theta + y \sin \theta - r) dx dy, \quad (12)$$

where δ denotes the Dirac delta-distribution. The function $(r, \theta) \mapsto P_\theta(r)$ is called the Radon transform of f . The main result that allows reconstruction of f from its Radon transform is the Fourier slice theorem, which relates the 2D Fourier transform of f to the 1D Fourier transform P_θ : for a given angle θ , let $\omega \mapsto \widehat{P}_\theta(\omega)$ be the 1D Fourier transform of $r \mapsto P_\theta(r)$ and $(u, v) \mapsto \widehat{f}(u, v)$ the 2D Fourier transform of f . One reads [36]

$$\widehat{P}_\theta(\omega) = \widehat{f}(u, v), \quad (13)$$

where (u, v) is the frequency that belongs to the radial line passing through the origin with angle θ and which is located at distance ω from the origin : $u = \omega \cos \theta$, $v = \omega \sin \theta$.

Since only a finite number of line integrals can be measured, the function \widehat{f} is known for a limited number of points (u, v) , which are radial points since they are distributed among a polar grid (see Fig. 1). Notice that the density of radial points becomes sparser as one gets farther away from the center that is, when one considers higher frequency components. A straightforward image reconstruction in the frequency domain can be sketched as follows : using a 1D Discrete Fourier Transform (DFT), the sequence $(\widehat{P}_\theta(\omega))_\theta$ is computed for all measured angles θ ; the non-uniformly spaced data $(\widehat{f}(u, v))_{(u,v)}$ are then interpolated to a uniform Cartesian grid; afterwards, the inverse Fourier transform is computed using a 2D inverse DFT. Thanks to the efficiency of the Fast Fourier Transform (FFT), such approach, called Direct Fourier Method (DFM), requires only $O(N^2 \log N)$ arithmetic operations for an image of size $N \times N$.

The main drawback of frequency domain reconstruction remains the occurrence of visual artifacts, due especially to inaccuracies in the high frequency band. The approach comes up against two difficulties [37] : the interpolation to

perform in the frequency space [38] and sharp contours in the image producing Gibbs oscillations when high frequencies are missing. Therefore, the standard reconstruction algorithm in clinical application, which is the filtered backprojection (FBP), does not work on the frequency domain but on the spatial one. The reconstruction is done by applying a ramp filter and by summing over the image plane the inverse Fourier transforms of the filtered projections [36]. The back-projection computes for each pixel in the reconstructed image the sum of all line integrals that pass through that pixel, and requires therefore $O(N^3)$ arithmetic operations.

The goal of our application is not to propose one of the fastest algorithms, but rather to introduce a method which offers better reconstructed images than standard ones, while its computational cost remains in the $O(N^2 \log N)$ (or $O(N^3)$) bound. The idea is to formulate the image reconstruction issue as a constrained optimization problem in the frequency space, the constraints being the knowledge of $(\widehat{f}(u, v))$ in the polar grid while the functional to minimize will be chosen in order to eliminate visual artifacts. Although such formulation appears to be new in tomographic imaging, optimization methods have already been proposed, especially in the spatial-domain approach. Let A denote the discrete Radon transform and s the sinogram. A common optimization formulation is

$$\min_f \|Af - s\| \quad (14)$$

where the norm is usually the quadratic one. The solution is found iteratively using, for example, the conjugate gradient algorithm. This requires to efficiently compute both A and its adjoint operator and it can be done in $O(N^2 \log N)$ using one of the fast Radon transform algorithms [39] or by sparse matrix multiplication. A frequency-domain version of (14) has been proposed by Bronstein *et al.* in [40] in the context of diffraction ultrasound tomography. In this case A is a projection operator in an oversampled Fourier basis, computed using a non-uniform Fourier transform [41], while s is the projection of the sinogram. The authors propose to incorporate into the solution some types of *a priori* information, using the Tikhonov-regularized form [5]

$$\min_f \|Af - s\| + \lambda\phi(f) \quad (15)$$

where ϕ is the regularization functional, and where the parameter λ controls the tradeoff between a good fit to the data and the smoothness of the solution.

3.2 TV in computerized tomography

Classical norms such as the quadratic one are not well-suited to be used as the regularization functional ϕ , since they tend to reconstruct images with blurred edges. For tomographic images, the most meaningful visual information is given by the shape of the objects (such as tumors), and therefore edges and enclosed areas have to be reconstructed sharply and without artifact. As the TV functional penalizes oscillations but not sharp discontinuities, the BV set appears to constitute a particularly relevant space of analysis.

We propose therefore the choice $\phi = \text{TV}$, and we adapt our simple TV-minimization framework to the ill-posed problem of tomographic imaging. Solving this problem formulated in the Fourier domain leads implicitly to solve the polar to Cartesian interpolation, in an optimal way regarding the BV image model. To the best of our knowledge, other approaches using TV-minimization in the Fourier domain are up to now limited to extrapolation and interpolation of the spectrum [30][42] in order to enhance image resolution (zoom). One may consider our method as a very particular case of spectrum extrapolation and interpolation, where known and missing values follow a specific geometry. Up to now, only a very few articles combines TV with tomography reconstruction [40] [43]. These two works do not consider a constrained problem as we do, but rather an unconstrained one like the formulation (15), and they do not apply to x-ray parallel beams tomography (although they probably could be adapted to). A very recent article [44] introduces the TV in the context of binary tomography : it is used to enforce a set of constraints while the energy to minimize is the quadratic error with the FBP reconstructed image.

3.3 Definition of the constraint

Let $P_\theta(r)$ be the sinogram, given at the grid points

$$(r_k, \theta_l) := (k \cdot \Delta r, l \cdot \Delta \theta); \quad k = -\frac{K}{2}, \dots, \frac{K}{2} - 1; \quad l = 0, \dots, L - 1; \quad \Delta \theta = \frac{\pi}{L}. \quad (16)$$

Adapting the Fourier slice theorem (13) to the discrete setting and using L univariate DFT of length K , we get

$$S_{k,l} := \widehat{P}_{\theta_l}(\omega_k) = \Delta r \sum_{s=-\frac{K}{2}}^{\frac{K}{2}-1} P_{\theta_l}(r_s) e^{-2\pi j \cdot \frac{sk}{K}}. \quad (17)$$

They are 2D-Fourier coefficients of the image f we have to reconstruct. However, these coefficients are given over the polar grid

$$Q_{k,l} := (\omega_k, \theta_l) \quad (18)$$

and in order to perform the bivariate inverse DFT, we must guess frequency coefficients over the Cartesian grid

$$C_{m,n} := (m \Delta x, n \Delta x) \quad (19)$$

of size $N \times N$. Let $(F_{m,n})$ be those Fourier coefficients.

The constraint space (10) may be rewritten as

$$U = \left\{ f \in \mathbb{R}^{N^2} : \quad \forall m, n = -\frac{N}{2}, \dots, \frac{N}{2} - 1, \quad F_{m,n} \in [F_{m,n}^-, F_{m,n}^+] \right\}, \quad (20)$$

where the bounds $[F_{m,n}^-, F_{m,n}^+]$ are computed over a polar neighborhood using a local Lipschitz regularity assumption.

3.4 Polar neighborhood

By allowing frequency $F_{m,n}$ to freely vary inside $[F_{m,n}^-, F_{m,n}^+]$, one permits to smooth the reconstructed image regarding to the TV functional. The geometry of polar neighborhood has to be designed with care : on one side, neighborhoods should not be too wide in order to use all known information. On the other side, they should not be too narrow so that the algorithm could be able to smooth the image enough to remove the noise. We consider disks of constant radius r and centered at coordinates (m, n) of the Cartesian grid. Over the polar grid, points representing low frequencies are dense enough, whereas high frequency points are sparse (see Fig. 1). For coordinates (m, n) near the origin, the disk neighborhood might include too many polar points and so the constraint $[F_{m,n}^-, F_{m,n}^+]$ may be too large. We therefore limit the number of polar points to a fixed integer M , see Fig. 2. More precisely, the disk neighborhood of $C_{m,n}$ is defined by

$$V_{m,n} = \{(k, l) : d(Q_{k,l}, C_{m,n}) < r\}, \quad (21)$$

the list of points (k, l) being ordered in increasing distance from $C_{m,n}$ and limited to at most M points. At high frequency it may exist (m, n) such that $V_{m,n} = \emptyset$ and $F_{m,n}$ cannot be recovered by the knowledge of its neighborhood. In such a case we do not set any constraint on (m, n) , and therefore highest frequencies are reconstructed by means of TV spectral extrapolation [42]. Experiments show that parameters r and M may be fixed to $r = 3$ and $M = 40$; they do not appear to depend of the image. As the FFT requires the number of samples to be a power of two, projection data are zero-padded before computing the 1D transform of every row. This operation generates a denser polar grid and this pre-interpolation eases to get non-empty $V_{m,n}$ at high frequencies. Accordingly, the Cartesian grid is oversampled by reducing the interval of frequency samples.

3.5 Local Lipschitz regularity

We compute bounds $F_{m,n}^-, F_{m,n}^+$ on each neighborhood $V_{m,n}$ using a local Lipschitz assumption. As the Shepp-Logan phantom is made by piecewise-constant functions, its Fourier transform is a combination of cardinal sine functions and is therefore, in the continuous model, infinitely many times differentiable. However, real sinograms suffer from noise and the hypothesis $\hat{f} \in C^\infty$ would be surely unrealistic. We believe however that assuming f to be locally Lipschitz continuous is a reasonable condition, and such a weak assumption would be enough to compute intervals bounds. On each $V_{m,n}$, we estimate the Lipschitz constant by

$$L_{m,n} = \max_{(k,l),(k',l') \in V_{m,n}} \frac{|S_{k,l} - S_{k',l'}|}{d(Q_{k,l}, Q_{k',l'})}, \quad (22)$$

and we define the intervals bounds by averaging deviations from all known values in the neighborhood :

$$F_{m,n}^\pm = \begin{cases} \frac{1}{\#V_{m,n}} \sum_{(k,l) \in V_{m,n}} S_{k,l} \pm L_{m,n} d(Q_{k,l}, C_{m,n}) & \text{if } V_{m,n} \neq \emptyset, \\ \pm\infty & \text{if } V_{m,n} = \emptyset. \end{cases} \quad (23)$$

3.6 Experimental results

With the above definitions and $T = 2\text{D-FFT}$, the algorithm sketched in Section 2.2 is applied to reconstruct CT images. To start the algorithm, one may choose $f^0 = \text{image reconstructed by DFM or by FBP}$. As r and M are fixed, the only remaining parameter is the number of iterations K (or, equivalently, the constant c used to define step-sizes $t_k = \frac{c}{k+1}$) and Fig.3 tells us that K should be chosen small, leading to a fast algorithm : pre-computation of the constraint space U needs $O(N^2)$ operations while other computations are of the same order of the FFT, that is $O(N^2 \log N)$. The overall complexity of our algorithm remains therefore in the same complexity class than the standard algorithm used to compute f^0 ($O(N^2 \log N)$ with DFM, $O(N^3)$ with FBP).

We have experimented the algorithms on the Shepp and Logan head phantom, for which projection data have been computed using a discrete Radon transform. Several image sizes have been checked, but in the following we only report experiments corresponding to $N = 256$. We set $\Delta r = \Delta x$ so there are $K = \sqrt{2} \times N \approx 367$ parallel beams for each angle. In order to reconstruct the image reliably [36], the number of angles L is chosen to be N . Each row of projection data are zero-padded to obtain the size $K = 1024$ and the Cartesian grid is oversampled to the size 512×512 . Without any noise, all algorithms perform well with visually almost indistinguishable differences, but our constrained-TV method is the one that achieves the highest PSNR. However in real tomography, noise is always disturbing the reconstruction process. As noticed in [45], inverting a noisy Radon transform is a hard task since the Radon transform is a smoothing operator and projections have, roughly speaking, one-half derivative more smoothness than the original image. The most used method, windowed FBP, exhibits degradation in recovering f from noisy data, since high-frequency components are considered as noise and the reconstruction is done mainly with low-frequency ones. Our approach allows to keep the information in the high-frequency bands while the noise is removed by the action of the TV functional. As a result of, our algorithm clearly outperforms classical ones when noise is added to the Radon transform. Fig. 4 shows simulation results in the presence of Gaussian white noise in the sinogram. The following algorithms have been experimented : DFM with linear interpolation in the Fourier space; plain FBP; FBP with Hamming filter to reduce the noise; ROF-like approach (space-based Tikhonov regularization (15) with $\phi = \text{TV}$); and at last our constrained-TV framework. The efficiency of DFM and plain FBP in presence of noise is very poor, with noisy reconstructed images. Applying a Hamming window with FBP increases noticeably the visual quality, by reducing the noise without altering edges (removing more high-frequencies would decrease the noise further, but edges would be smoothed). TV-regularization using Tikhonov model performs well in denoising data, but the image is slightly blurred by the relaxation (5) and by the absence of strong constraints. Best results are by far obtained with our constrained-TV minimization method, that denoises the image without significantly affecting edges. Also, the PSNR is much greater than the other ones and surprisingly than the ROF-like one (with a difference greater than 3 db).

We believe that, by projecting on a *had hoc* constraint space, our algorithm is able to denoise data without affecting too much edges (compare plots of ROF versus constrained-TV in Fig.4 : the noise amplitude is greater with ROF while main peaks - corresponding to the white ellipse - are lower).

Besides, in order to obtain fair results with ROF one has to perform a much greater number of iterations (30 in our experiment). As already noted in the beginning our algorithm, although convergent, exhibits best results after a small number of iterations only (7 in our experiment, see Fig.3). Indeed, if in the first steps the algorithm tends to reduce the noise and oscillatory artifacts (ringing), after a while the TV functional is known to produce staircase effects and to erode peaks [46][47][48]. The constraint we are using protects somewhat from this phenomenon, but is too weak in highest frequencies to avoid it completely.

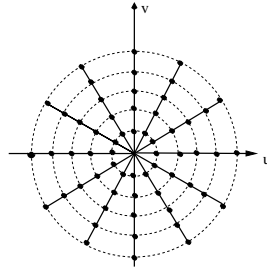


Fig. 1. Points (u, v) where $\hat{f}(u, v)$ is known are distributed among a polar grid, they are therefore radial points. Due to this particular geometry, the density of radial points becomes sparser when frequencies are increasing : reconstruction of missing high frequency components is the major issue of tomographic imaging.

References

1. Rudin, L., Osher, S., Fatemi, E.: Nonlinear total variation based noise removal algorithms. *Physica D* **60** (1992) 259–268
2. Chambolle, A., Lions, P.L.: Image recovery via total variation minimization and related problems. *Numer. Math.* **76** (1997) 167–188
3. Acar, R., Vogel, C.: Analysis of total variation penalty methods for ill-posed problems. *Inverse Problems* **10** (1994) 1217–1229
4. Li, Y., Santosa, F.: A computational algorithm for minimizing total variation in image restoration. *IEEE Trans. on Image Proc.* **5** (1996) 987–995
5. Vogel, C., Oman, M.: Iterative method for total variation denoising. *SIAM J. Sci. Comput.* **17** (1996) 227–238
6. Dobson, D.C., Vogel, C.R.: Convergence of an iterative method for total variation denoising. *SIAM J. Numer. Anal.* **34** (1997) 1779–1791
7. Vogel, C., Oman, M.: Fast, robust total variation-based reconstruction of noisy, blurred images. *IEEE Trans. on Image Proc.* **7** (1998) 813–824

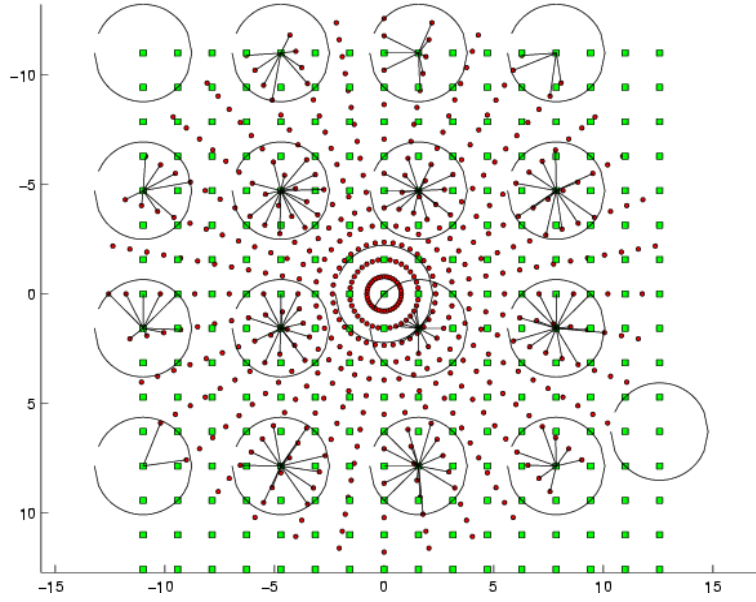


Fig. 2. The disk neighborhoods with $r = \sqrt{2}$ and $M = 16$ (these values are for illustration). Points $Q_{m,n}$ of the polar grid are marked as black dots while points $C_{m,n}$ of the Cartesian one are marked as grey squares.

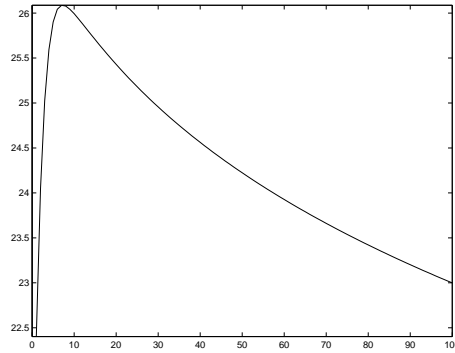


Fig. 3. PSNR versus number of iterations. The quality of the reconstructed image is firstly rapidly increasing, and decreases after a given threshold has been reached. This optimal number of iterations is 3 for noiseless images and increases with the quantity of noise, but does not exceed 10. This graph corresponds to the experiment reported in Fig. 4 (last line), with noise level $\text{SNR}=20.1$. The same kind of graph has been obtained with any implementation of our constrained-TV framework, including examples of Section 2.3.

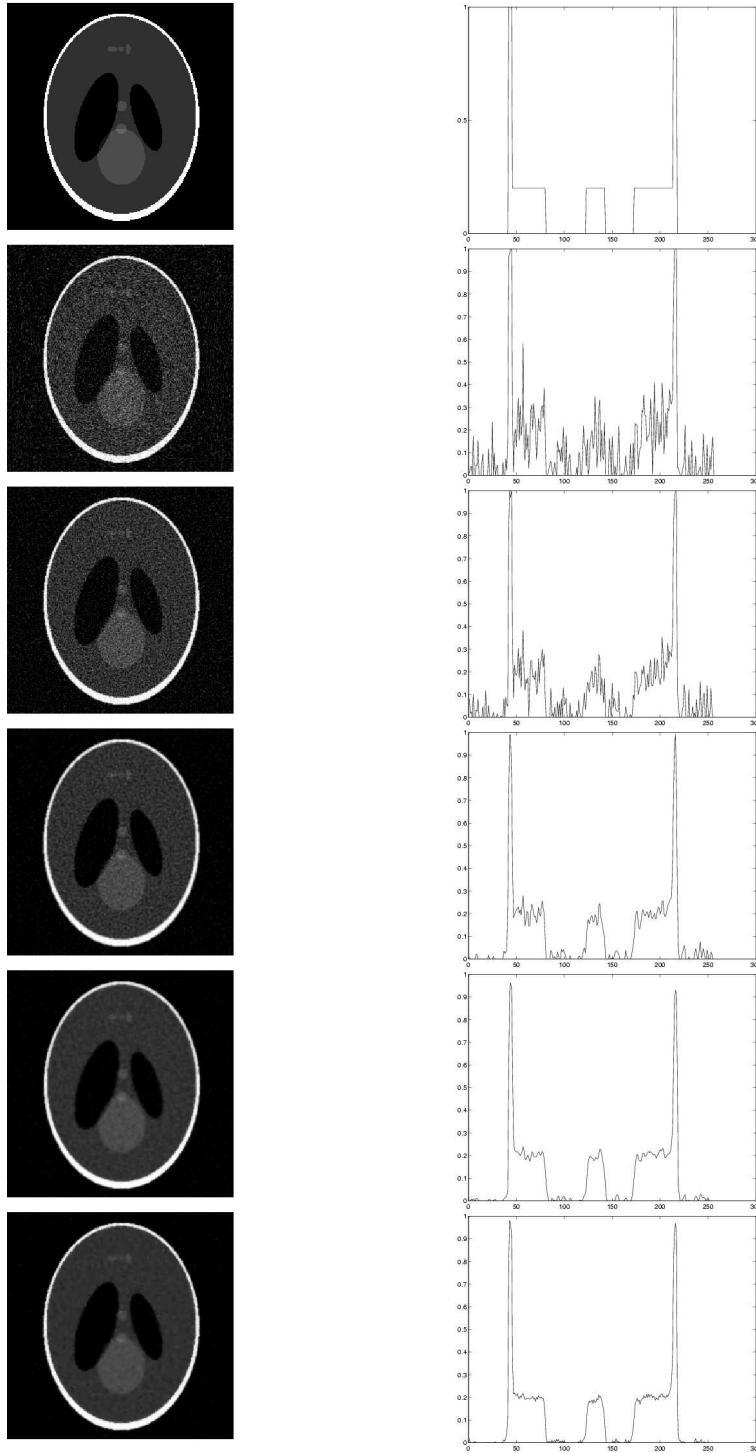


Fig. 4. Reconstruction with noisy data added on the sinogram (noise level: SNR=20.1). Left column : reconstructed images. Right column : plots of an horizontal section (located at the middle of the image). Lines, from up to down : original Shepp-Logan phantom; DFM with linear interpolation (PSNR=20.3); FBP (PSNR=22.4); FBP with Hamming window (PSNR=24.1); ROF (PSNR=22.9, 30 iterations); our constrained-TV algorithm (PSNR=26.1, 7 iterations).

8. Chan, T., Golub, G., Mulet, P.: A nonlinear primal-dual method for total variation-based image restoration. *SIAM J. Sci. Comput.* **20** (1999) 1964–1977
9. Dibos, F., Koepfler, G.: Global total variation minimization. *SIAM J. Numer. Anal.* **37** (2000) 646–664
10. Darbon, J., Sigelle, M.: Exact optimization of discrete constrained total variation minimization problems. In Klette, R., Zunic, J., eds.: Tenth International Workshop on Combinatorial Image Analysis. *Lecture Notes in Computer Science* 3322 (2004) 548–557
11. Combettes, P., Luo, J.: An adaptive level set method for nondifferentiable constrained image recovery. *IEEE Trans. on Image Proc.* **11** (2002) 1295–1304
12. Durand, S., Froment, J.: Reconstruction of wavelet coefficients using total variation minimization. *SIAM J. Sci. Comput.* **24** (2003) 1754–1767
13. Chambolle, A.: An algorithm for total variation minimization and applications. *J. Math. Imaging Vis.* **20** (2004) 89–97
14. Alter, F., Durand, S., Froment, J.: Deblocking dct-based compressed images with weighted total variation. In: Proc. of ICASSP 2004, Montréal. Volume 3. (2004)
15. Coifman, R., Sowa, A.: Combining the calculus of variations and wavelets for image enhancement. *Applied and Comput. Harmonic Ana.* **9** (2000) 1–18
16. Chan, T.F., Zhou, H.: Total variation improved wavelet thresholding in image compression. In: Proc. of ICIP'2000. (2000)
17. Malgouyres, F.: Combining total variation and wavelet packet approaches for image deblurring. In: Proc. of IEEE work. on VLSM 2001, Vancouver, Canada. (2001) 57–64
18. Malgouyres, F.: Minimizing the total variation under a general convex constraint for image restoration. *IEEE Trans. on Image Proc.* **11** (2002) 1450–1456
19. Aliney, S.: A property of the minimum vectors of a regularizing functional defined by means of the absolute norm. *IEEE Trans. on Signal Proc.* **45** (1997) 913–917
20. Nikolova, M.: Minimization of cost-functions with non-smooth data-fidelity terms to clean impulsive noise. In Rangarajan, A., Figueiredo, M.A.T., Zerubia, J., eds.: *EMMCVPR*. Volume 2683 of *Lecture Notes in Computer Science.*, Springer (2003) 391–406
21. Nikolova, M.: Minimization of cost-functions involving nonsmooth data-fidelity terms. application to the processing of outliers. *SIAM J. Numer. Anal.* **40** (2002) 965–994
22. Gousseau, Y., Morel, J.M.: Are natural images of bounded variation ? *SIAM J. Math. Anal.* **33** (2001) 634–648
23. Meyer, Y.: Oscillating patterns in image processing and in some nonlinear evolution equations. In: The Fifteenth Dean Jacqueline B. Lewis Memorial Lectures. Volume 22., American Mathematical Society (2001)
24. Osher, S., Solé, A., Vese, L.: Image decomposition and restoration using total variation minimization and the h^{-1} norm. *SIAM Multiscale Model. Simul.* **1** (2003) 349–370
25. Vese, L., Osher, S.: Image denoising and decomposition with total variation minimization and oscillatory functions. *J. Math. Imaging Vis.* **20** (2004) 7–18
26. Aujol, J., Aubert, G., Blanc-Féraud, L., Chambolle, A.: Image decomposition into a bounded variation component and an oscillating component. *J. Math. Imaging Vis.* **22** (2005)
27. Aujol, J., Chambolle, A.: Duals norms and image decomposition models. *Int. Jour. of Computer Vision* **63** (2005) 85–104
28. Alter, F., Durand, S., Froment, J.: Adapted total variation for artifact free decomposition of jpeg images. *J. Math. Imaging Vis.*, to appear (2005)

29. Shepp, L., Logan, B.: The fourier reconstruction of a head section. *IEEE Trans. Nucl. Sci.* **21** (1974) 21–43
30. Guichard, F., Malgouyres, F.: Total variation based interpolation. In: *Proc. of EUSIPCO'98*. Volume 3. (1998) 1741–1744
31. Polyak, B.: *Introduction to Optimization*. Optimization Software (1987)
32. Combettes, P.L.: Convex set theoretic image recovery by extrapolated iterations of parallel subgradient projections. *IEEE Trans. on Image Proc.* **6** (1997) 493–506
33. Durand, S., Froment, J.: Artifact free signal denoising with wavelets. In: *Proc. of ICASSP'01*, Salt Lake City. Volume 6. (2001)
34. Donoho, D., Johnstone, I.: Ideal spatial adaptation via wavelet shrinkage. *Biometrika* **81** (1994) 425–455
35. Wallace, G.: The jpeg still picture compression standard. *Communications of the ACM* **34** (1991) 31–44
36. Kak, A., Slaney, M.: *Principles of Computerized Tomographic Imaging*. SIAM (2001)
37. Gottlieb, D., Gustafsson, B., Forssén, P.: On the direct fourier method for computer tomography. *IEEE Trans. Medical Imaging* **19** (2000) 223–232
38. Waldén, J.: Analysis of the direct fourier method for computer tomography. *IEEE Trans. Medical Imaging* **19** (2000) 211–222
39. Averbuch, A., Coifman, R., Donoho, D., Israeli, M., Waldén, J.: Fast slant stack: A notion of radon transform for data in a cartesian grid which is rapidly computable, algebraically exact, geometrically faithful and invertible. *SIAM J. Sci. Comput.* (to appear)
40. Bronstein, M., Bronstein, A., Zibulevsky, M., Azhari, H.: Reconstruction in ultrasound diffraction tomography using non-uniform fft. *IEEE Trans. Medical Imaging* **21** (2002) 1395–1401
41. Fessler, J., Sutton, B.: Nonuniform fast fourier transforms using min-max interpolation. *IEEE Trans. on Signal Proc.* **51** (2003) 560–574
42. Moisan, L.: Extrapolation de spectre et variation totale pondérée. In: *Proc. of GretsI'01*, Toulouse, France. (2001)
43. Jonsson, E., Huang, S., Chan, T.: Total variation regularization in positron emission tomography. UCLA CAM Report 98-48, University of California, Los Angeles, CA, <http://www.math.ucla.edu/~chan/papers.html> (1998)
44. Capricelli, T.D., Combettes, P.L.: Parallel block-iterative reconstruction algorithms for binary tomography. In: *Special issue of Electronic Notes in Discrete Mathematics : Workshop on discrete tomography and its applications*, June 13-15, 2005, New York City, Elsevier (to appear)
45. Lee, N.Y., Lucier, B.J.: Wavelet methods for inverting the radon transform with noisy data. *IEEE Trans. on Image Proc.* **10** (2001) 79–94
46. Chan, T., Marquina, A., Mulet, P.: High-order total variation-based image restoration. *SIAM J. Sci. Comput.* **22** (2000) 503–516
47. Dobson, D., Santosa, F.: Recovery of blocky images from noisy and blurred data. *SIAM J. Appl. Math.* **56** (1996) 1181–1199
48. Durand, S., Malgouyres, F., Rougé, B.: Image deblurring, spectrum interpolation and application to satellite imaging. *ESAIM:COCV Control, Opt. and Cal. of Var.* **5** (2000) 445–475